ORIGINAL RESEARCH ARTICLE

Current Research on Biosciences and Biotechnology **7** (1) 2025 27-34

Current Research on Biosciences and Biotechnology

www.crbb-journal.com

Development of an efficient and eco-friendly method for mitragynine enrichment

Rizal Febriandi[a], Defri Rizaldy[a], Sumail Sidik Ode Ishak[ab], Elfahmi[ac*]

[a]School of Pharmacy, Bandung Institute of Technology, Bandung, West Java, Indonesia
[b]EBM Scitech Research Center, EBM Scientific and Technology Ltd., Bandung, West Java, Indonesia
[c]University Center of Excellence for Nutraceuticals, Biosciences and Biotechnology Research Center, Bandung Institute of Technology, Bandung, West Java, Indonesia

ABSTRACT

Kratom (*Mitragyna speciosa*) is rich in mitragynine, a bioactive alkaloid with antinociceptive, sedative, and antimicrobial activities, and potential benefits for alleviating alcohol dependence. This study aimed to develop a safe, environmentally friendly, cost-effective, and efficient method for enriching mitragynine using macroporous resins. Extraction was performed via maceration with 70% ethanol, and the performance of macroporous resins (PAD610 and PAD900) was evaluated in terms of adsorption and desorption characteristics using UPLC-MS/MS. The results showed that the adsorption and desorption processes followed a pseudo-second-order kinetic model, indicating that mitragynine adsorption is influenced by coexisting compounds in the extract. Isothermal adsorption analysis demonstrated good agreement with the Freundlich model, with R^2 values of 0.9973 for PAD610 and 0.9905 for PAD900, suggesting multilayer adsorption on heterogeneous surfaces. Under optimized conditions, macroporous resin enrichment effectively increased mitragynine content, yielding 753 mg for PAD900 and 303 mg/g for PAD610. Additionally, a flow rate of 3 BV/hour was identified as optimal for large-scale applications. This study demonstrates that macroporous resins provide an efficient and scalable approach for mitragynine enrichment from *M. speciosa* extract, offering a promising method for the preparation of high-purity bioactive compounds.

Article history:

Received 14 Mar 2025
Revised 20 Aug 2025
Accepted 24 Aug 2025
Available online 31 Aug 2025

Keywords:

Mitragyna speciosa
mitragynine
macroporous resin
LC-MS
green extraction

*Corresponding authors:
elfahmi@itb.ac.id

DOI: 10.5614/crbb.2025.7.1/362C71GB

e-ISSN 2686-1623/

1. Introduction

Kratom plant (*Mitragyna speciosa*), a member of the Rubiaceae family, is taxonomically related to the coffee plant (Akbar et al., 2023). Traditionally, kratom leaves have been utilized for a range of ethnomedicinal purposes, including as wound poultice, antipyretic, muscle pain reliever, appetite suppressant, and antidiarrheal agent. Recent studies have expanded upon these empirical uses, demonstrating that kratom leaves exhibit diverse pharmacological activities, including analgesic, stimulant, antidepressant, antioxidant, anti-inflammatory, antinociceptive, and antibacterial properties (Juanda et al., 2019).

Mitragynine, the predominant indole alkaloid isolated from *M. speciosa* leaves, has shown significant analgesic potential through its modulation of opioid receptors, offering promise for pain management with a lower risk of adverse effects compared to morphine (Karunakaran et al., 2022). The concentration of mitragynine in *M. speciosa* varies according to geographic origin and harvest conditions. Notably, kratom from Thailand contains up to 66% mitragynine of total alkaloids, while Malaysian varieties typically contain approximately 12% (Amrianto et al., 2021).

Several methodologies for the extraction and isolation of mitragynine have been reported, each with distinct advantages and limitations. However, most existing fractionation and isolation techniques rely on organic solvents such as *n*-hexane, ethyl acetate, and methanol, which are hazardous to human health and detrimental to the environment. This highlights the need for safer, more sustainable, and efficient approaches to mitragynine isolation. One promising strategy involves the application of macroporous polymer resins (Beng et al., 2011).

Macroporous resins offer an effective and environmentally benign platform for the purification and enrichment of bioactive compounds at industrial scale. Commercially available resins include aromatic types (polydivinylbenzene) and aliphatic types (polymethacrylic) (Yang et al., 2022). Among these, polydivinylbenzene microparticles exhibit superior binding capacity compared to gel-type resins and possess a permanently porous architecture, making them suitable for a wide range of applications (Garcia-Diego and Cuellar, 2005). These characteristics suggest that macroporous resin-based methodologies hold significant potential for the eco-friendly and efficient isolation of mitragynine from *M. speciosa*.

2. Materials and methods

2.1. Materials

The materials used in this study included PAD610 and PAD900 macroporous resins for the adsorption of mitragynine compounds

from *Mitragyna speciosa* extract. The dried powdered simplicia of *M. speciosa* was extracted using the maceration method with 70% ethanol for 24 hours, repeated three times. The combined extracts were filtered and evaporated to dryness using a rotary evaporator at 50 °C. The dried extract was analyzed for mitragynine content and subsequently applied to macroporous resins to evaluate the adsorption and desorption capacities. All analyses were performed using a UPLC-MS/MS system.

2.2. MRM optimization of mitragynine

Multiple Reaction Monitoring (MRM) parameters for mitragynine were optimized using a UPLC-ESI-MS/MS instrument equipped with an electrospray ionization (ESI) source operating in positive ionization mode. Optimization of precursor and product ions (m/z) was performed, considering dwell time, cone voltage (V), and collision energy (V). Additional parameters—including capillary voltage, source temperature, desolvation temperature, desolvation gas (nitrogen), and collision gas (argon)—were optimized for enhanced sensitivity and specificity. Data acquisition and processing were performed using MassLynx software.

2.3. UPLC-MS/MS method validation

Mitragynine quantification was performed using UPLC-MS/MS with gradient elution. The stationary phase was a C_{18} column, while the mobile phase consisted of water with 0.1% formic acid and acetonitrile with 0.1% (v/v) formic acid. The flow rate was maintained at 300 µL/min, and detection was performed in MRM mode. The method was validated for linearity, limit of detection (LOD), limit of quantification (LOQ), specificity, accuracy, and precision to ensure analytical reliability.

2.4. Extract preparation

Powdered *M. speciosa* samples were extracted by maceration with 70% ethanol for 24 hours, repeated three times. The combined extracts were filtered and evaporated to dryness at 50 °C using a rotary evaporator. A portion of the dried extract was analyzed for mitragynine content using the validated UPLC-MS/MS method.

2.5. Moisture content of adsorbent resins (PAD 900 and PAD 610)

Prior to use, resins were soaked in 95% ethanol for 24 hours, then thoroughly rinsed with distilled water using a chromatography column. The resins were weighed accurately, dried in an oven at 105 °C, and monitored until a constant weight was achieved to determine their moisture content.

2.6. Adsorption procedure

One gram of wet resin was placed in a 250 mL Erlenmeyer flask, and 25 mL of the prepared sample solution (dissolved in water) was added. The mixture was shaken in an orbital shaker at 130 rpm and 25 °C for 60 minutes. Aliquots of the supernatant were collected at 5-minute intervals, and mitragynine concentrations were analyzed using UPLC-MS/MS. The adsorption capacity and adsorption ratio of the resin were subsequently calculated.

2.7. Desorption procedure

Following adsorption, the resin was transferred to a 250 mL Erlenmeyer flask, and 25 mL of 70% ethanol was added. The mixture was shaken at 130 rpm for 60 minutes. Samples were collected at 5-minute intervals and analyzed via UPLC-MS/MS to determine desorption capacity and desorption ratio.

2.8. Isothermal adsorption of *M. speciosa* extract solution

A series of extract solutions with varying mitragynine concentrations were prepared and placed in Erlenmeyer flasks. The mixtures were shaken at 130 rpm at room temperature until equilibrium was achieved. Samples were analyzed using UPLC-MS/MS, and adsorption isotherms were evaluated using Langmuir and Freundlich models.

2.9. Dynamic adsorption/desorption

For dynamic studies, resins were packed into a column, washed sequentially with ethanol and distilled water, and loaded with extract solutions at flow rates of 2, 3, and 4 bed volumes (BV)/hour. Samples were collected every 10 minutes and stored for subsequent UPLC-MS/MS analysis. Desorption was performed using ethanol at varying concentrations (20-90% v/v) with a bed volume of 1. The collected eluent fractions were analyzed by UPLC-MS/MS to determine mitragynine content.

3. Results and discussion

3.1. MRM optimization

Multiple reaction monitoring (MRM) is widely utilized for compound detection due to its high selectivity and sensitivity, enabling the development of an accurate UPLC-MRM/MS analytical method (El-Hawiet et al., 2022). MRM optimization for mitragynine was performed based on its fragmentation pattern using direct infusion with ESI-MS/MS. The ionization mode employed was electrospray ionization (ESI) in positive ionization mode (ESI+), allowing for the detection of both parent and daughter ions.

Mass detection optimization in ESI-positive mode (M+H) was conducted under the following conditions: capillary voltage of 3.00 kV, source temperature of 150 °C, nitrogen gas flow rate of 900 L/hour, cone voltage of 55 V, and collision energy of 30 V. Under these optimized parameters, the characteristic m/z ratios for mitragynine were successfully determined (Table 1).

3.2. Optimal conditions for chromatographic system

In addition to MRM optimization, chromatographic conditions were optimized to ensure accurate and reproducible UPLC performance. Key parameters optimized included the mobile phase composition (gradient profile), mobile phase pH, flow rate, and column temperature.

Table 1. MRM detection parameters for mitragynine

Compound	Parent ion (m/z)	MRM transition		Cone Voltage (V)	Collision energy (V)	
		Quantifier (m/z)	Qualifier (m/z)		Quantifier (m/z)	Qualifier (m/z)
Mitragynine	399.25	110.18	174.20	55	30	30

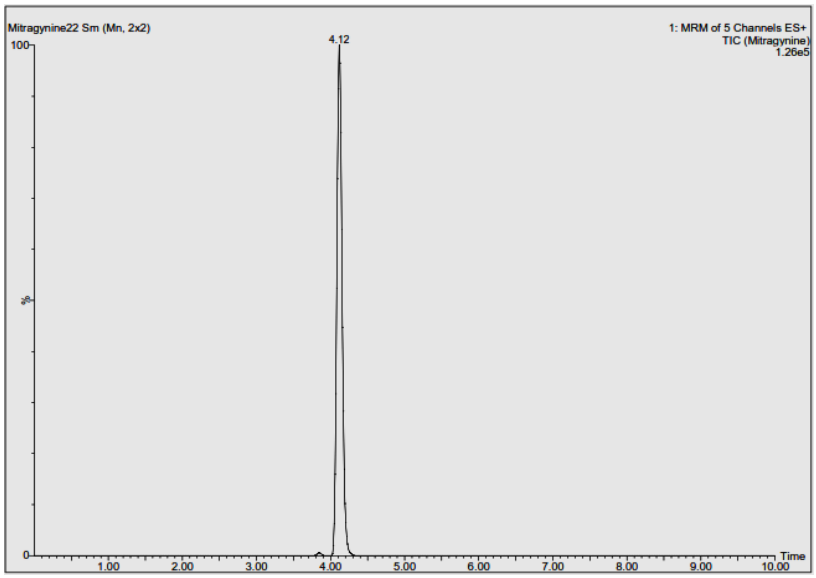

Fig. 1. Chromatogram MRM of mitragynine

Chromatographic separation was achieved using an Acquity UPLC® BEH C_{18} column (1.7 µm, 2.1 × 100 mm). The mobile phase consisted of Solvent A (water with 0.1% formic acid) and Solvent B (acetonitrile with 0.1% formic acid). The optimized gradient program was as follows:

- 0.00–1.0 min: 10–20% B
- 1.0–3.0 min: 20–50% B
- 3.0–5.0 min: 50% B
- 5.0–5.10 min: 50–100% B
- 5.10–10.0 min: 100% B

The flow rate was maintained at 0.3 mL/min, with an injection volume of 3 µL and a column temperature of 40 °C. These optimized conditions produced a well-resolved chromatographic profile of mitragynine, as illustrated in Fig. 1.

3.3. Linearity

Linearity testing, or standard curve validation, is performed to determine whether an analytical method produces results that are directly proportional to the analyte concentration within the tested range (Ambarati et al., 2023). For linearity validation, six concentration levels of mitragynine standards were prepared: 3.125, 1.563, 0.781, 0.391, 0.195, and 0.098 ppm. Each concentration was analyzed in triplicate using ultra-high-performance liquid chromatography (UHPLC).

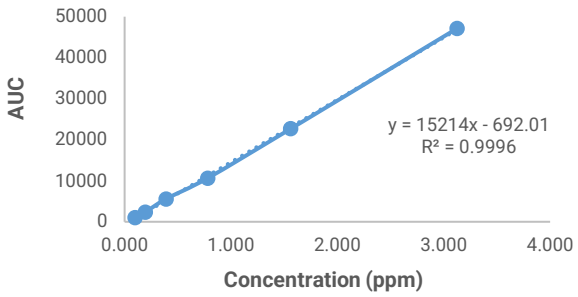

Fig. 2. Calibration curve of mitragynine

As shown in Fig. 2, the method yielded a determination coefficient (R^2) of 0.9996, exceeding the acceptance criterion of $R^2 \geq 0.995$ (Suhendi and Ramly, 2021), indicating excellent linearity of the analytical method within the tested concentration range.

3.4. Limit of detection (LOD) and Limit of quantification (LOQ).

Following the establishment of the calibration curve for mitragynine, the limit of detection (LOD) and limit of quantification (LOQ) were determined. LOD represents the lowest analyte concentration that can be reliably detected by the analytical method but does not need to be quantified as an exact value. Conversely, LOQ is the lowest analyte concentration that can be quantified with acceptable accuracy and precision (Nugraheni and Anggoro, 2016). The results demonstrated that the method exhibited high sensitivity for mitragynine detection. The calculated detection and quantification limits were 0.004 ppm for LOD and 0.013 ppm for LOQ, respectively (Table 2).

Table 2. Instrument detection limit and method quantification limit

AUC	Standard deviation response	Limit of detection (ppm)	Limit of quantification (ppm)
246.112			
237.193			
271.728			
298.058	20.074	0,004	0.013
271.352			
274.025			
259.599			

3.5. Determination of resin moisture content.

The moisture content of the aromatic (PAD 900) and aliphatic (PAD 610) macroporous resins was determined using the gravimetric method. Both resins were soaked in 96% ethanol for 24 hours to remove residual monomers and porogenic agents trapped in the pores during synthesis. Subsequently, the resins were thoroughly rinsed with distilled water using a chromatography column to ensure complete removal of impurities.

The resins were then accurately weighed, placed in a drying oven, and dried at 105 °C until a constant weight was achieved. The analysis revealed that the moisture content was approximately 74.20% for PAD 900 and 73.06% for PAD 610. Based on these values, the actual dry mass per gram of wet resin was calculated as 258.041 mg for PAD 900 and 269.354 mg for PAD 610 (Table 3).

Table 3. Moisture content of macroporous aromatic (PAD 900) and aliphatic (PAD 610) resins

Resin	Resin wet weight (g)	Resin dry weight (g)	Resin moisture content (%)	Average (%)
PAD 900	1.0881	0.2760	76.4731	74,1959 ± 1.7153
	1.0137	0.2733	73.0394	
	1.0325	0.2748	73.3818	
PAD 610	1.0216	0.2813	72.4680	73.0646 ± 0.6020
	1.0140	0.2670	73.6719	
	1.0333	0.2784	73.0540	

3.6. Adsorption ratio and capacity of PAD 610 and PAD 900 resins for mitragynine solution

The adsorption ratio and capacity tests were performed to evaluate the ability of aromatic macroporous resins to bind mitragynine. An initial solution was prepared at a concentration of 10 mg in 25 mL, and aliquots were collected at five-minute intervals to monitor adsorption kinetics.

The results demonstrated that both PAD 610 and PAD 900 resins effectively adsorbed mitragynine; however, PAD 900 exhibited superior performance. PAD 610 reached adsorption equilibrium in 35 minutes, achieving an adsorption capacity of 3.64 mg/g and an adsorption ratio of 63.15%. In contrast, PAD 900 reached equilibrium more rapidly, within 15 minutes, with an adsorption capacity of 4.38 mg/g and an adsorption ratio of 99.86% (Fig. 3).

The enhanced performance of PAD 900 is attributed to its higher adsorption capacity and faster equilibrium rate. An ideal adsorbent is characterized by high capacity, rapid adsorption kinetics, and robust mechanical and chemical stability. Furthermore, the surface area of the resin plays a critical role in adsorption efficiency, as larger contact areas facilitate greater adsorption capacity (Zhang et al., 2014).

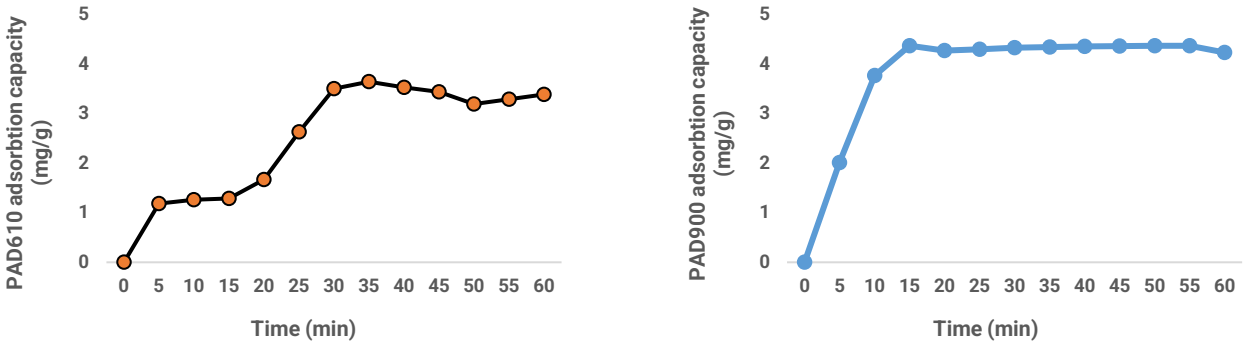

Fig. 3. Adsorption capacity of PAD 610 (left) and PAD 900 (right) towards mitragynine

3.7. Desorption capacity of PAD 610 and PAD 900 resins for mitragynine

Desorption capacity refers to the efficiency of a solvent in releasing compounds bound to an adsorbent. To evaluate the desorption performance of the resins, 25 mL of 70% ethanol was added to the resins that had previously undergone the adsorption process. The mixtures were agitated at 120 rpm for 60 minutes, and aliquots were collected at regular intervals to monitor desorption kinetics.

As shown in Fig. 4, PAD 610 resin reached desorption equilibrium at 25 minutes, achieving a desorption capacity of 2.113 mg/g and a desorption ratio of 57.91%. In contrast, PAD 900 resin reached equilibrium more rapidly, within 15 minutes, with a desorption capacity of 3.83 mg/g and a desorption ratio of 96.48%. These findings indicate that PAD 900 exhibits superior desorption efficiency compared to PAD 610. However, the use of 70% ethanol did not achieve complete desorption, likely due to strong chemical interactions between mitragynine molecules and the resin matrix. This suggests that optimizing the desorption solvent composition could further enhance recovery efficiency.

3.8. Adsorption/desorption kinetics of resins towards *M. speciosa* extract

Adsorption kinetics studies are conducted to elucidate the mechanisms governing interactions between compounds and the surface of an adsorbent. Several kinetic models, including pseudo-first-order, pseudo-second-order, the Elovich equation, and intraparticle diffusion kinetics, are commonly applied to characterize adsorption and desorption behavior.

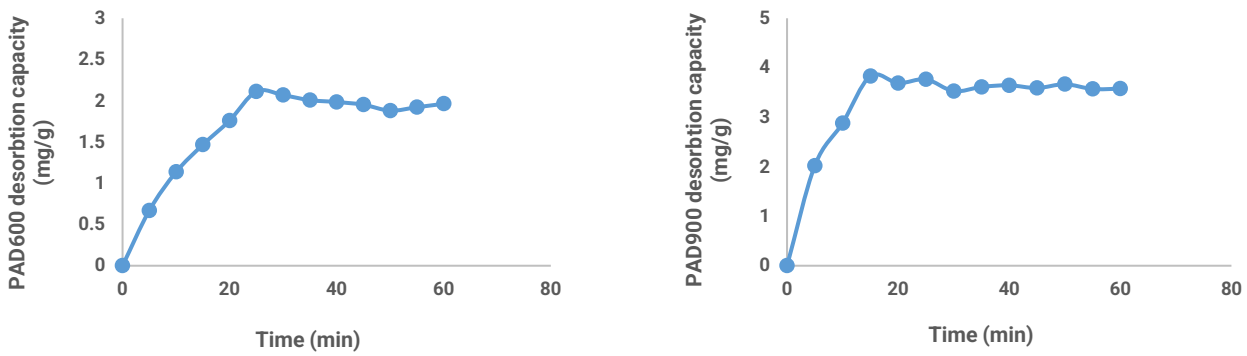

Fig. 4. Desorption capacity of PAD 610 (left) and PAD 900 (right) towards mitragynine

Table 4. Adsorption kinetic parameters

Resin	Adsorption Kinetic Parameters	Value parameters
PAD 610	Pseudo Orde 1	y = -0.1299x+8.736
	k_1 (1/min)	-0.1299
	R^2	0.9713
	Pseudo Orde 2	y = 0.0002x + 0.0006
	k_2 [mg/(g min)]	0.0002
	R^2	0.9931
	Elovich	y = 1175.1x + 1559.4
	α [mg/(g min)]	1175.1
	R^2	0.8141
	Difusi Intrapartikel	y =-0.1333x+954.11
	k_{id} [mg/(g min$^{1/2}$)]	-0.1333
	R^2	0.8420
PAD 900	Pseudo Orde 1	y = -0.0977x + 8.9588
	k_1 (1/min)	-0.0977
	R^2	0.9647
	Pseudo Orde 2	y = 0.0001x - 5E-06
	k_2 [mg/(g min)]	0.0001
	R^2	0.9993
	Elovich	y = 2019.8x - 486.58
	α [mg/(g min)]	2019.8
	R^2	0.8033
	Difusi Intrapartikel	y = 1.0311x - 6925
	k_{id} [mg/(g min$^{1/2}$)]	1.0311
	R^2	0.9227

In this study, adsorption kinetics were evaluated using an *M. speciosa* extract solution to investigate the interactions between the adsorbent and the bioactive compounds. Analysis of the kinetic parameters provided insights into the adsorption mechanisms of mitragynine on the resins. The calculated adsorption kinetic parameters for the resins are summarized in Table 4.

The adsorption and desorption kinetics of mitragynine on PAD610 and PAD900 macroporous resins were investigated to elucidate the mechanisms governing compound-resin interactions. Adsorption experiments were conducted using an *M. speciosa* extract solution prepared by dissolving 0.32 g of extract in 25 mL of water (0.8 mg/mL mitragynine). The mixtures were agitated, and aliquots were collected at five-minute intervals for analysis using UPLC-MS/MS.

Kinetic modeling was performed using pseudo-first-order, pseudo-second-order, Elovich, and intraparticle diffusion equations. As summarized in Table 4, the pseudo-second-order model exhibited an R^2 value closest to 1, indicating that adsorption of mitragynine is influenced not only by the target compound but also by coexisting constituents in the extract, such as polyphenols and glycosidic flavonoids. The lower R^2 value for the Elovich model, which predicts chemisorption, suggests that chemisorption contributes minimally to the adsorption process. This indicates that adsorption is predominantly governed by physical interactions, influenced by factors such as initial adsorbate concentration, temperature, pH, resin surface area, and the composition of the solution matrix (Ho, 2006).

Experimental results demonstrated that PAD900 resin outperformed PAD610, achieving adsorption equilibrium faster and with higher capacity. PAD610 reached equilibrium at 25 minutes with an adsorption capacity of 6.092 mg/g, whereas PAD900 achieved equilibrium in 20 minutes with a capacity of 7.033 mg/g (Fig. 5).

Desorption studies using 70% ethanol revealed that equilibrium was reached after 10 minutes, with PAD900 exhibiting a desorption capacity of 10.71 mg/g of dry resin and a desorption ratio of 99.71%, exceeding that of the pure mitragynine solution. This enhanced desorption is likely due to the nature of the physical interactions between mitragynine and the resin. Van der Waals forces, which include dipole–dipole interactions, dipole–induced dipole interactions, and dispersion forces (London forces), play a dominant role in physical adsorption (Lima et al., 2015). Dispersion forces, being weak and easily reversible, are likely responsible for the higher desorption ratio of mitragynine in the extract solution, as these interactions facilitate efficient release from the resin matrix.

Overall, these findings indicate that PAD900 resin provides superior adsorption and desorption performance for mitragynine in *M. speciosa* extract, demonstrating rapid kinetics, high capacity, and nearly complete recovery. The study underscores the importance of resin selection, surface properties, and solution composition in optimizing adsorption/desorption processes for bioactive compounds from complex plant matrices.

3.9. Isotherm adsorption of *M. speciosa* extract

The adsorption behavior of mitragynine on PAD610 and PAD900 resins was evaluated using the Langmuir and Freundlich isotherm models, which describe the interactions between the sorbent and adsorbate and are useful for assessing adsorption linearity and solute–resin interactions. As shown in Fig. 6, the adsorption capacity of both resins increased with increasing initial concentration of mitragynine.

Data were fitted to the Langmuir and Freundlich equations to characterize equilibrium interactions. The analysis revealed that the Freundlich model provided a better fit for both resins, with R^2 values of 0.9973 for PAD610 and PAD900. The Freundlich model assumes that adsorption capacity increases with adsorbate concentration and that adsorption can occur on multiple layers, theoretically allowing for unlimited adsorption (Lima et al., 2015).

The model's acceptance criteria require a standard deviation (SD) ≤ 13.21. The obtained SD values were 4.37 for PAD610 and 3.59 for PAD900, indicating an excellent fit. These results suggest that the adsorption of mitragynine on both aromatic macroporous resins follows the Freundlich isotherm, confirming multilayer adsorption behavior and heterogeneous surface interactions.

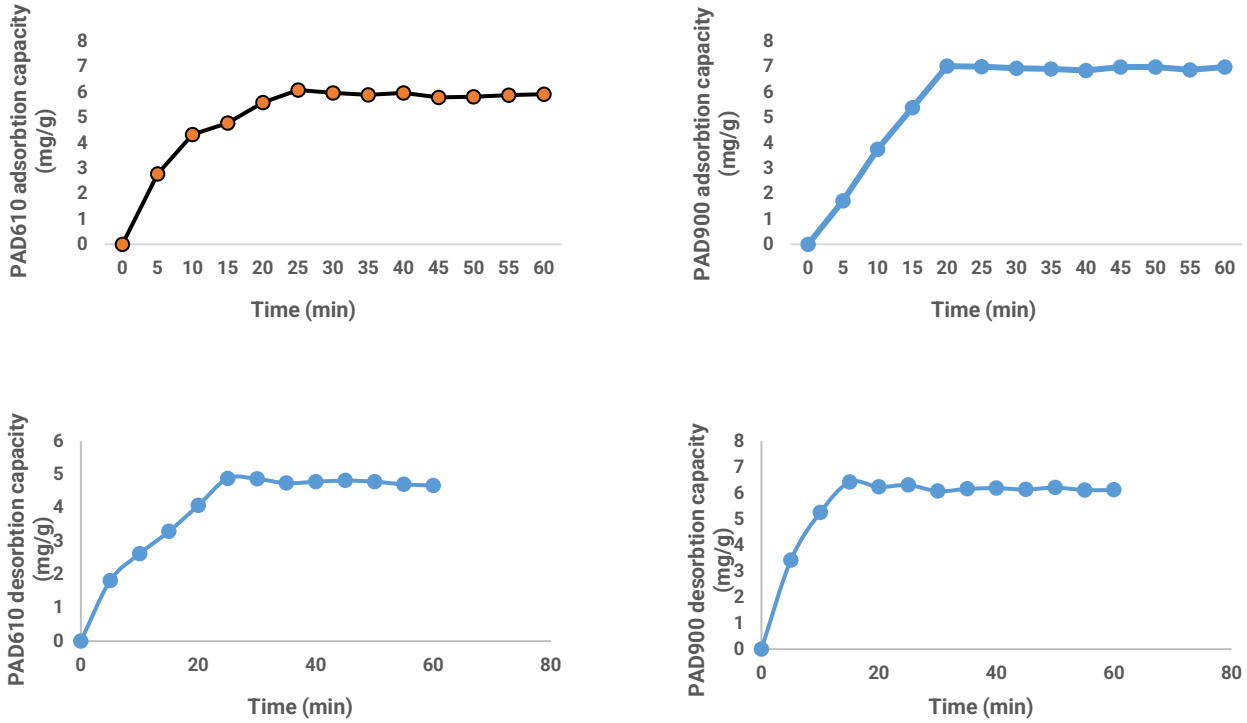

Fig. 5. Adsorption and desorption capacity of resins for Mitragynine in *M. speciosa* extract solution

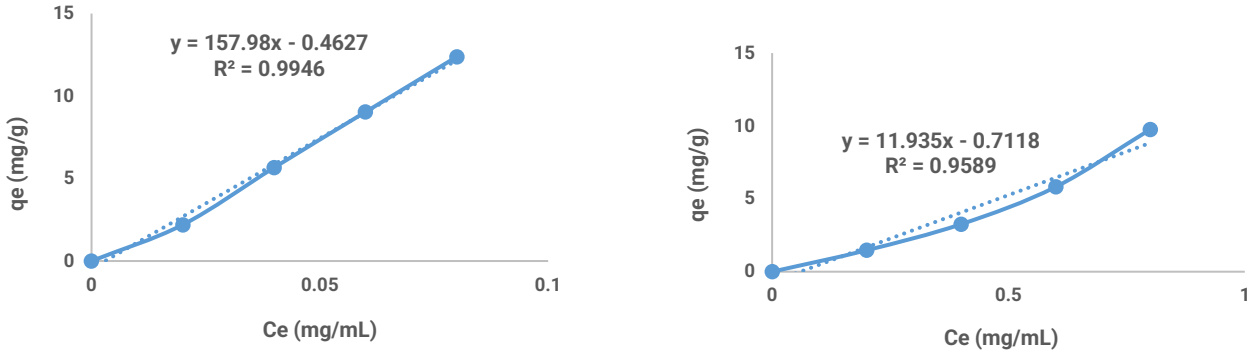

Fig. 6. Isotherm adsorption of PAD610 (left) dan PAD900 (right) towards *M. speciosa* extract

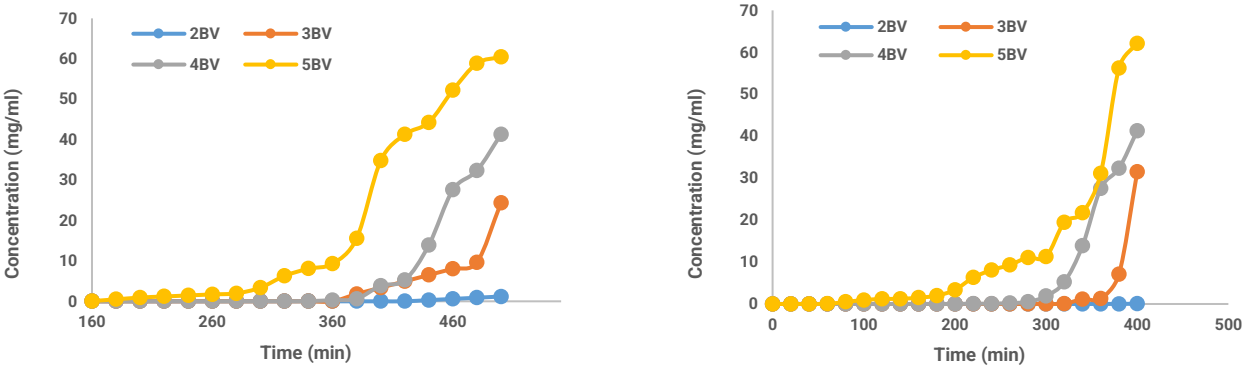

Fig. 7. Dynamic adsorption of PAD610 (left) dan PAD900 (right) towards *M. speciosa* extract

3.10. Adsorption dynamics of *M. speciosa* extract

Dynamic adsorption experiments were conducted using a laboratory-scale column (21 cm length × 3 cm diameter) packed with 15 g of aromatic macroporous resin (bed volume, 30 mL) to evaluate the breakthrough behavior of mitragynine. The *M. speciosa* extract solution (0.8 mg/mL mitragynine) was loaded into the column at various flow rates of 2, 3, 4, and 5 BV/h.

Breakthrough curves were generated to analyze the dynamic characteristics of the resin column, providing insights for optimizing and designing large-scale purification processes. As shown in Fig. 7, the breakthrough point varied with flow rate. Faster

flow rates resulted in earlier breakthrough, indicating that the time to reach saturation is inversely proportional to flow velocity. Conversely, slower flow rates allowed more mitragynine to be adsorbed before breakthrough, reflecting improved adsorption efficiency.

Based on the data, an optimal flow rate of 3 BV/h was identified for large-scale purification, achieving a total adsorbed mitragynine amount of 237 mg (Table 5). These results highlight the importance of controlling flow rate in column design to balance adsorption efficiency and process throughput.

3.11. Dynamic desorption of *M. speciosa* extract

Dynamic desorption of mitragynine was investigated to evaluate the effects of elution parameters, including solvent flow rate, ethanol concentration, and column geometry. Prior to elution, the resin-packed column was washed with 3 BV of deionized water and then eluted with 1 BV of ethanol solution ranging from 20-90% (v/v). Desorption efficiency increased at 40-60% ethanol but declined at higher concentrations (70-90%).

As shown in Fig. 8, lower flow rates resulted in higher desorption efficiency due to longer contact time between the desorption solvent and the adsorbed compounds. Specifically, a flow rate of 2 BV/h achieved higher desorption at 70-90% ethanol, while 3 BV/h optimized desorption efficiency at 90% ethanol, which was therefore selected as the optimal elution rate.

Despite optimization, the overall recovery of mitragynine under dynamic desorption conditions was lower than that observed in static desorption, particularly for PAD610 (57% recovery) compared to PAD900 (96% recovery). This reduced recovery is likely due to co-elution of other compounds present in the extract. Previous studies report that young *M. speciosa* leaves contain multiple indole alkaloids, including mitragynine, speciogynine, paynantheine, and speciociliatine, as well as minor alkaloids such as 7-hydroxy-7H-mitragynine, mitragynaline, pinoresinol, mitralactonal, and mitrasulgynine, which may interfere with mitragynine adsorption and desorption (Hassan et al., 2013).

Table 5. Flow rate and breakthrough point relationship

Resin	Flow (bv)	Leakage point (min)	Adsorbed mitragynine (mg)
PAD 610	5	160	193
	4	280	229
	3	340	303
	2	420	266
PAD 900	5	60	475
	4	200	568
	3	280	753
	2	360	660

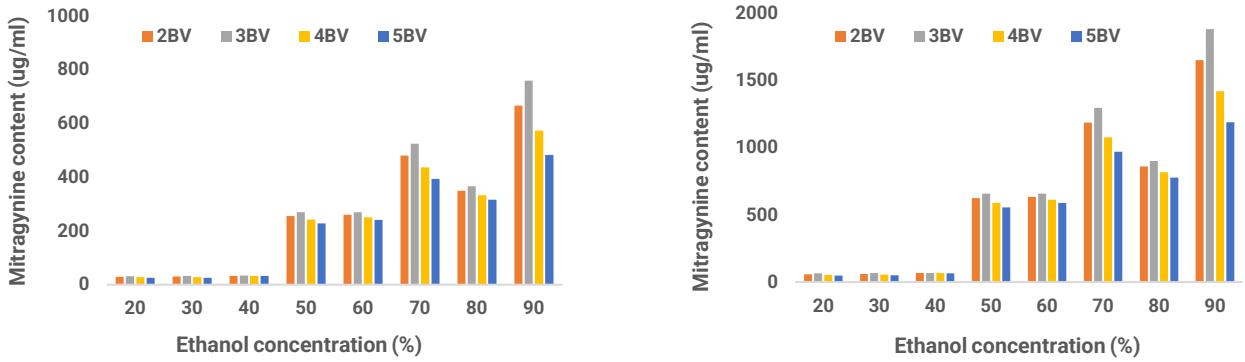

Fig. 8. Dynamic desorption of PAD610 (left) and PAD900 (right) towards mitragynine in extract using ethanol

4. Conclusion

The results of this study demonstrate that mitragynine enrichment from *M. speciosa* extract can be effectively achieved using macroporous resins PAD900 and PAD610. Method validation confirmed the analytical reliability of mitragynine quantification, with a linearity regression coefficient of 0.9996, a limit of detection (LOD) of 0.004 ppm, and a limit of quantification (LOQ) of 0.013 ppm. The macroporous resins were characterized by moisture contents of 74.20% (PAD900) and 73.06% (PAD610), supporting their suitability for adsorption and desorption applications.

Acknowledgements

Authors gratefully acknowledge the Ministry of Education, Culture, Research and Technology for a research grant under the scheme of “Penelitian Thesis Magister 2024”.

Conflict of interest

The authors declare no conflict of interest in this research.

References

Akbar MAS, Pratiwi DE, Salempa P. 2023. Isolation and identification of secondary metabolic compounds ethyl acetate fraction of kratom plant stem (*Mitragyna speciosa*) (in Indonesian). *Jurnal Chemica* 24(1): 1-8. doi: 10.35580/chemica.v24i1.35501

Ambarati T, Wahyudi YN, Indratno SHA, Nurfadhila L. 2023. Review article: Validation of analytical methods for the determination of paracetamol levels in biological samples using various methods (in Indonesian). *J Pharm Sci* 6(2): 838-847. doi: 10.36490/journal-jps.com.v6i2.157

Amrianto, Ishak SSO, Putra N, Salsabila S, Al Muqarrabun LMR. 2021. Mitragynine: a review of its extraction, identification, and purification methods. *CRBB* 3(1): 165-171. doi: 10.5614/crbb.2021.3.1/TMPNSA4H

Beng GT, Hamdan MR, Siddiqui MJ, Mordi MN, Mansor SM. 2011. A simple and cost effective isolation and purification protocol of mitragynine from *Mitragyna speciosa* Korth (Ketum) leaves (in Indonesia). *Malays J Anal Sci* 15(1): 54-60.

El-Hawiet A, Elessawy FM, El Demellawy MA, Amira El-Yazbi AF. 2022.

Green fast and simple UPLC-ESI-MRM/MS method for determination of trace water-soluble vitamins in honey: Greenness assessment using GAPI and analytical eco-scale. *Microchem J* 181: 107625. doi: 10.1016/J.Microc.2022.107625

Garcia-Diego C, Cuellar J. 2005. Synthesis Of Macroporous Poly(Styrene-Co-Divinylbenzene) Microparticles Using N-Heptane As The Porogen: Quantitative Effects Of The Dvb Concentration And The Monomeric Fraction On Their Structural Characteristics. *Ind Eng Chem Res* 44(22): 8237-8247. doi: 10.1021/ie050091e

Hassan Z, Muzaimi M, Navaratnam V, Yusoff NHM, Suhaimi FW, Vadivelu R, Vicknasingam BK, Amato D, von Hörsten S, Ismial NIW, Jayabalan N, Hazim AI, Mansor SM, Müller CP. 2013. From kratom to mitragynine and its derivatives: Physiological and behavioural fffects related to use, abuse, and addiction. *Neurosci Biobehav Rev* 37(2): 138-151. doi: 10.1016/j.neubiorev.2012.11.012.

Ho YS. 2006. Review of second-order models for adsorption systems. *J Hazard Mater* 136(3): 681-689. doi: 10.1016/j.jhazmat.2005.12.043

Juanda E, Andayani S, Maftuch. 2019. Phytochemical screening and antibacterial activity of kratom leaf (*Mitragyna speciosa* Korth.) against *Aeromonas hydrophilla*. *J Exp Life Sci* 9(3): 155-158. doi: 10.21776/ub.jels.2019.009.03.02

Karunakaran T, Ngew KZ, Zailan AAD, Jong VYM, Bakar MHA. 2022. The chemical and pharmacological properties of mitragynine and its diastereomers: An insight review. Front Pharmacol 13: 805986. doi: 10.3389/Fphar.2022.805986

Lima E, Adebayo MA, Machado FM, Lima EC, Adebayo MA, Machado FM, Lima EC. 2015. Chapter 3: Kinetic and equilibrium models of adsorption. In: Bergmann CP, Machado FM (Ed.). Carbon nanomaterials as adsorbents for environmental and biological applications. Germany: Springer International Publishing, p. 33-69. doi: 10.1007/978-3-319-18875-1_3

Nugraheni B, Anggoro AB. 2016. Validation of ciprofloxacin analysis method using High Performance Liquid Chromatography (HPLC) (in Indonesian). *Jurnal Inovasi Teknik Kimia* 1(1): 06-08. doi: 10.31942/inteka.v1i1.1638

Suhendi A, Ramly EA. 2021. Validation of rifampicin capsule analysis method using HPLC-PDA (in Indonesian). *Farmasains Jurnal Ilmiah Ilmu Kefarmasian* 8(1): 31-36. doi: 10.22236/farmasains.v8i1.5602

Yang X, Zhao R, Wang H, Ben A. 2022. Resin adsorption as a means for the enrichment and separation of three terpenoid indole alkaloids: Vindoline, catharanthine and vinblastine from *Catharanthus roseus* extracts in ionic liquid solution. *Ind Crops Prod* 187: 115351. doi: 10.1016/J.Indcrop.2022.115351

Zhang M, Li A, Zhou Q, Shuang C, Zhou W, Wang M. 2014. Effect of pore size distribution on tetracycline adsorption using magnetic hypercrosslinked resins. *Micropor Mesopor Mater* 184: 105-111. doi: 10.1016/j.micromeso.2013.10.010